Investigation into effect of cosmic radiation on microstructural parameters and optical properties of the lower atmosphere in middle and high latitudes.

Part 1. Influence of a charge on heterogeneous processes in the atmosphere

L.S. Ivlev and S.N. Khvorostovskii

Scientific Research Institute of Physics at St.-Petersburg State University

Received July 17, 2000

The influence of an electric charge on the growth of aerosol particles under background atmospheric conditions is investigated. In this investigation, the permanently acting ionizing factors are taken into account, as well as the size distribution of aerosol particles. The fraction of particles whose size is larger than the critical one and its dependence on the value and sign of the charge are determined.

Introduction

The effect of solar radiation on the state of the lower atmosphere, its temperature and radiative characteristics has long been one of the basic geophysical problems. Revealing the relation between the solar activity and variations of atmospheric parameters[1–5] is of special interest. Interpretation of this relation is very ambiguous, because variation of the net flux of solar energy at the top of the Earth's atmosphere is small in comparison with the energy of dynamic processes in the lower atmosphere. At the same time, it should be noted that such variations can be significant in some ranges of the solar energy flux, in particular, in flows of high-energy particles. Penetration of such particles into the atmosphere to its lower part leads to formation of a significant number of ions, excited molecules, and active radicals and favors appearance of a charge in aerosol particles. In this paper, we study the influence of these effects on the growth of primary particles and consider the processes leading to their formation.

1. Statement of the problem

The principal condition for formation of the disperse phase is the presence of supersaturated water vapor and so-called condensation nuclei, i.e., aerosol particles whose size is greater than some critical value, in the atmosphere. The models suggested in this paper assumes the following mechanisms of the influence of high-energy particles on the condensation process:

(1) Aerosol particles acquire a charge under the effect of an external flow of charged particles. The presence of even one elementary charge in a particle leads to the decrease of the critical size of aerosol particles which can serve as nuclei for condensation and sublimation of water vapor or other condensing gases. Hence, more aerosol particles are involved into heterogeneous condensation.[6] It should be also noted that the sign of the charge affects the condensation activity of a particle.[7]

(2) The process of ionization of atmospheric molecules leads to formation of new easily condensing gaseous components, which independently form condensation nuclei, i.e., homogeneous heteromolecular condensation is observed. Such components are, first of all, water vapor and sulfur and nitrogen oxides. Ozone, atomic oxygen, hydroxyl, and some other radicals take an active part in chemical and photochemical reactions.

Thus, growth of primary aerosol particles due to both homogeneous and heterogeneous condensation and coagulation growth at the high particle number density[6] are possible in lower atmospheric layers under the effect of cosmic rays. Obviously, the character of formation a cloud layer depends on the concentrations and composition of the initial products (gases and aerosol particles), intensity of the flow of high-energy particles of space origin, their characteristics in the considered atmospheric layer, and thermodynamic characteristics of this layer. Formation of a cloud system is considered here to mean the increase of the optical thickness of a certain atmospheric layer by an order of magnitude and more in comparison with the background value.

In this paper, we deal with only the possibilities of formation of cloud systems at heterogeneous condensation under the effect of high-energy charged particles in the atmospheric layers from 8 to 30 km in middle and high latitudes. For this purpose, we have to analyze the conditions of interaction of high-energy particles with aerosol and gaseous components of the atmosphere at the height from 8 to 30 km.

2. Effect of an electric charge on growth of aerosol particles under background atmospheric conditions

Let us consider the effect of an electric charge on the growth of aerosol particles in the absence of the intense flow of high-energy particles in the atmosphere. It is well-known that the heterogeneous mechanism of condensation of water vapor or other condensing gases, which requires the presence of condensation nuclei (Aitken nuclei) in the atmosphere, is always more efficient than the homogeneous one. For particles to grow by this mechanism, the intensity of adsorption of vapor molecules on the particle surface must be higher than the intensity of desorption. That is, there must exist forces efficiently preventing desorption of vapor molecules.[6]

One of the possible mechanisms of decreasing the intensity of desorption of vapor molecules is electrostatic interaction of vapor molecules, especially, the easy polarized water molecule, with the charge of an aerosol particle.[7] The growth condition is fulfilled, if the saturation pressure of water vapor above a particle is lower than the partial vapor pressure in the surrounding air. The relative humidity f_0 at the equilibrium state of the vapor above the charged droplet is expressed by the refined Thomson (Kelvin) equation in the form derived by Rusanov[8]:

$$f_0(a) = \frac{P_{\text{sat}}(a)}{P_\infty(\infty)} = \exp \frac{1}{\rho kT}\left[\frac{2\sigma(a)}{a} - \frac{1}{8\pi}\left(\frac{1}{\varepsilon^\beta} - \frac{1}{\varepsilon^\alpha}\right)\frac{q^2}{a^4}\right], \quad (1)$$

where ρ, σ, and ε^α are the density, specific surface tension, and dielectric constant of water, respectively; ε^β is the dielectric constant of water vapor; a and q are the radius and charge of a droplet, respectively. The maximum value $f_{0\max}$ is observed at $a_{\text{cr}} = \sqrt[3]{q^2(1/\varepsilon^\beta - 1/\varepsilon^\alpha)/4\pi\sigma}$. If the radius a is larger than a_{cr}, then the droplet becomes a stable nucleus at relative humidity less than 100%. However, already at the initial size of the particle $a > 1\cdot 10^{-5}$ cm the effect of the charge on the saturated vapor pressure above the particle is negligible, and the effect of the charge on the size of a stable nucleus is relatively weak ($a_{\text{cr}} \cong q$). So the mechanism of decreasing the saturation pressure above the solution – weak electrolyte (the Raoult law),[9] as well as the processes of condensate transition into other chemical (for example, sulfate) or phase (ice) states with lower saturation pressure is more efficient for particle growth to large size.

Condensation on concave surfaces of particles occurs at the partial pressure of the condensing vapor lower than the saturation pressure above the plane surface. However, we do not consider it here, because it relatively weakly affects the cross section of aerosol particles, i.e., almost does not increase scattering and extinction of solar radiation by particles. In the case of friable conglomerates (fractals), it even leads to the decrease of the particle cross section.

The electric charge can favor more effective coagulation growth of particles as well. However, relatively high concentrations of aerosol particles are necessary for this mechanism to occur. According to Smolukhowski, for Brownian coagulation $t_{\text{coag}} \cong 10^{10}\ \text{s}\cdot\text{cm}^{-6}/N^2$. Hence, this process becomes essential in the actual atmosphere only at $N > 10^3\ \text{cm}^{-3}$. The aerosol polydispersity (presence of giant particles with $a > 1\ \mu$m) and existence of large charges ($q > 10e$) in some particles favor coagulation. Calculations show that the effective coagulation coefficients of unlikely charged particles can be higher, and, hence, the coagulation lifetime is one order of magnitude or even more shorter than that for uncharged particles ($t_{\text{coag}} \cong 10^3$–$10^2$ s at $N > 10^3\ \text{cm}^{-3}$). The effective coagulation coefficients of likely charged particles are close to that of uncharged particles at high charge ratios.[6]

The distribution of the electric charge of aerosol particles in the atmosphere undisturbed by high-energy particles was calculated in a number of papers.[10–12] These calculations were based on the Boltzmann distribution[12] with corrections for diffuse charging of particles at the known experimentally measured number densities of molecular ions in the air medium,[11] as well as with allowance made for the motion of ions and particles relative to each other (convective flows and fall of particles). In all the cases, the contribution of the impact mechanism of charging the aerosol particles is negligible in comparison with that of the diffusion one. According to Hann, the stationary electric charge in the particle of the radius a in the bipolarly charged atmosphere is determined as

$$q_0 = \frac{akT}{e} \ln \frac{n_+ D_+}{n_- D_-}, \quad (2)$$

where $n_\pm$ is the number density of molecular ions, and $D_\pm$ is their diffusion coefficient.

The calculated fractions of the charged aerosol particles of different size in the atmosphere $n_r(\pm p) = N_p/N_0 = \exp[-p^2 e^2/(2kTa)]$ are shown in Fig. 1. In calculations, we used the Boltzmann equation and equations by other authors that, in particular, more accurately take into account the ion flow on a sphere in a medium with the mean free path of a molecule comparable or greater than the aerosol particle size. The figure indicates that the fraction of charged particles with $a < 0.01\ \mu$m in the undisturbed bipolar atmosphere is small ($n \le 0.1$). This can be explained by the fact that the electric field strength E near the surface of a particle with the radius $a = 10^{-6}$ cm and the unit charge is equal to $1.4\cdot 10^5$ V/cm, and the discharge in the air medium occurs at $E = 2.8\cdot 10^4$ V/cm. The electrostatic energy of such a particle is equal to $1.1\cdot 10^{-13}$ erg, i.e., approximately twice as high as the kinetic energy of its thermal motion. Hence, the particles of the size $a < 0.01$ µm in the undisturbed atmosphere are not efficient condensation nuclei.

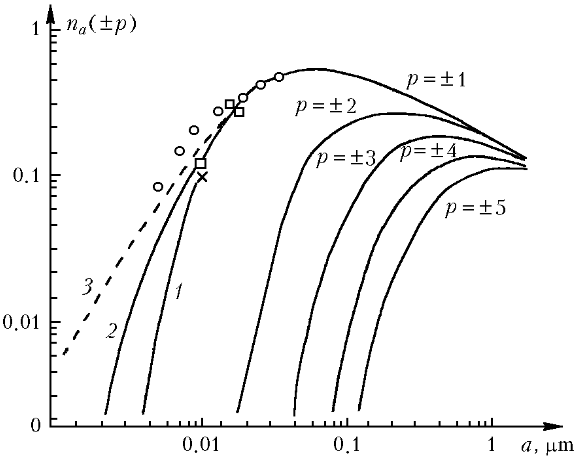

Fig. 1. Fraction of charged particles of different size $n_a(\pm p)$ with different charge: calculation by Boltzmann equation (*1*), Boltzmann and Kojime equation (*2*), and Hentry equations (*3*); ○, □, and × are experimental data of different authors.[10]

The particles of large size acquire larger charge according to the approximate equation $N/N_0 = 10\, a^{1/3}$. For example, q_0 of a particle with the size $a = 5$ µm is equal to $18e$ in the bipolar atmosphere and $84e$ in the unipolar one. In this case, efficient growth of particles can occur due to electrostatic coagulation. Allowance made for the effect of convective air motion on charging the aerosol particles and the falling rate of the aerosol particles leads to significant, by an order of magnitude or more, increase of the charge acquired by a particle starting from $r > 1$ µm. The maximum stationary charge in this case is determined as

$$q_{\mathrm{m}} = a^2 \frac{4kT}{e\lambda\pi} \frac{n_+^2\, u_+^2 - n_-^2\, u^2}{n_+^2\, u_+^2 + n^2\, u_-^2}, \tag{3}$$

where λ is the mean free path of molecules, $u_\pm = e\lambda/2m_\pm$ is mobility, and m_{++} is the mass of light ions. The characteristic time of achieving the equilibrium is determined as $t_0 = q_0/4\pi\, aD_\pm\, n_\pm$ and is about 10^2 s.

It should be noted that the effect of the particle charge on condensation properties is asymmetric with respect to the charge sign because of the strong polarizability of the water molecule. Water droplets and particles with a free water cover has a positive surface potential due to orientation of the water molecules and formation of the ion–dipole double layer. As a result, the energy of activation of the condensation process on negative centers is lower than that on the positive ones, i.e., negatively charged droplets grow more quickly.[7]

The problem of heterogeneous formation of nuclei in the presence of charges was studied by Klingo.[13,14] He has shown that the freezing point increased by about 20°C under the effect of a charge. That is, ice crystals are formed on the charged condensation nuclei in the actual atmosphere starting from the altitude of 5 km. The effect of the droplet (aerosol particle) charge on crystallization is caused by the increase of supersaturation of water vapor near the droplet surface, the decrease of the radius of an ice nucleus and the energy needed for its formation. The nucleation rate significantly depends on the ion size (the strength of its electric field).

3. Ionization rate and ion number density in the atmosphere in the absence of powerful flows of high-energy particles of space origin

The local rate of the ion formation in the atmosphere is the amount of ions formed for 1 s in 1 cm^3. In the near-ground atmospheric layer, it is determined by ionization of gas molecules by the background cosmic radiation and radioactive substances in the atmosphere and soil (mostly, radon and thoron). The radioactivity concentration of these elements near the ground is roughly the same (10^{-16}–10^{-15} Ci$\cdot$cm^{-3}). With height, it decreases slowly for radon (lifetime $\tau_{1/2}^{\mathrm{Ra}} \approx 3.8$ day) and rapidly for thoron ($\tau_{1/2}^{\mathrm{Th}} \approx 54$ s). The contributions of different factors to formation of ions near the ground are given in Table 1 (Ref. 15).

Table 1. Ionization rate in the atmosphere near the ground

Factor	Rate (amount of formed ion pairs, cm^{-3} s^{-1})
Cosmic rays	2
Radioactive substances in air	
α	4.4
β	0.03
γ	0.15
Radioactive substances in soil	
β	0.3
γ	3.2
Total	10.08

The mean amount of ion pairs formed for a monoenergetic α-particle is a determined value equal to $2\cdot 10^5$; for β- and γ-particles this value is determined very approximately and is roughly equal to $2\cdot 10^4$, i.e., one order of magnitude less.

Among decay products, mostly Th*B* ($\tau_{1/2} \approx 11$ hours) in the concentration of $19\cdot 10^{-4}$ cm^{-3} is observed in the background atmosphere. This concentration is of the same order of magnitude as the concentration of Ra*A* ($\tau_{1/2} \approx 3$ min) equal to $39\cdot 10^{-4}$ cm^{-3}.

Radioactive β- and γ-radiation of $2\cdot 10^{-18}$ Ci/cm^3 is observed near atom centers. This gives the ionization rate of $3\cdot 10^3$ cm$^{-3}\cdot$ s^{-1}.

In the troposphere, the contribution of ionization of air molecules by cosmic rays increases with height, and the contribution of radioactive substances, especially, of soil origin decreases sharply.

Since a water surface practically does not emit radioactive substances, the ionization rate above an ocean is less than that above continents. The mean ionization rate under background atmospheric conditions up to the height of 8–10 km is accepted to be equal to 10 $\text{cm}^{-3}\cdot\text{s}^{-1}$.

In the middle atmosphere, the ionization rate is completely determined by galactic cosmic rays.

At the altitude of the stratospheric aerosol layer, the globally mean ionization rate I_c is about 0.01 $\text{cm}^{-2}\cdot\text{s}^{-1}$. In winter it is approximately five times higher than in summer. In Ref. 15, the globally mean ionization rate in the entire atmospheric column is $9.3\cdot 10^2$ $\text{cm}^{-2}\cdot\text{s}^{-1}$ in winter and $1.6\cdot 10^2$ $\text{cm}^{-2}\cdot\text{s}^{-1}$ in summer.

In addition, the ionization rate increases with latitude due to the latitudinal behavior of the intensity of cosmic rays.

The ionization rate in the troposphere can increase significantly at emission of radioactive material of natural origin before an earthquake and at volcanic eruption. For example, as was estimated in Ref. 16, the radon emission before an earthquake can cause ionization with the rate about $7.6\cdot 10^3$ $\text{cm}^{-3}\cdot\text{s}^{-1}$, i.e., three orders of magnitude higher than the background value.

The ionization rate can be even greater at serious failures of atomic power plants. For example, the ionization rate in the layer of 50–100 m in the 30-km zone of the Chernobyl atomic power plant for the period of failure was 10^5–10^6 $\text{cm}^{-3}\cdot\text{s}^{-1}$ (Ref. 17).

Experimental investigations of the number density and chemical composition of atmospheric ions indicate that most ions contain 10 to 20 molecules of water, and their number density in the troposphere ranges as $n_\pm = 10^2$–10^4 cm^{-3} from 300–500 cm^{-3} at the ground level up to $(1–2)\cdot 10^4$ cm^{-3} in the altitude range from 8 to 30 km (Fig. 2). The ratio of positively charged ions to negatively charged ones is close to 1.2 under the background conditions.

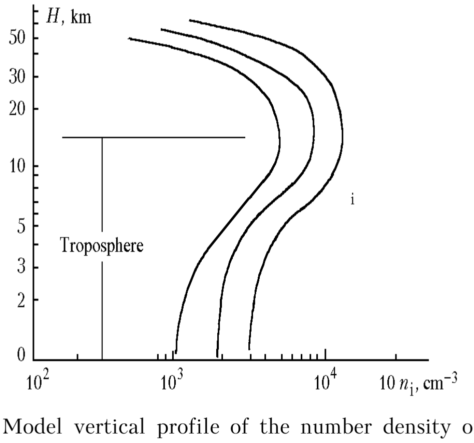

Fig. 2. Model vertical profile of the number density of light ions.[18]

Balloon-borne mass-spectrometric measurements in the altitude range from 8 to 30 km have revealed the following ions: $H^+(H_2O)_m$, $H^+(CH_3CN)_n(H_2O)_m$, $NO_3(HNO_3)_n$, and $HSO_4^-(H_2SO_4)_n(HNO_3)_n$.

According to Arnold,[18] $H^+(H_2SO_4)_n(H_2O)_m$ ions can form stable condensation nuclei in the altitude range from 30 to 50 km.

The ion concentration in the atmosphere is limited by both the ionization rate and the intensity of recombination processes, as well as their lifetime in the atmosphere τ_i. The lifetime of ions is determined by recombination of oppositely charged ions. It can be estimated as

$$\tau_i = (\alpha_i N_1)^{-1}, \tag{4}$$

where $\alpha_i = 1.6\cdot 10^{-6}$ $\text{cm}^{-3}\cdot\text{s}^{-1}$ is the ion recombination coefficient of light ions with an elementary charge. The lifetime of light ions depends on their capture by aerosol particles. This time is limited by ion flow and subsequent accommodation of ions on the surface of an aerosol particle. The ion flows depend on diffusion processes, electrostatic fields of regular air motions, and physicochemical properties of the surface of an aerosol particle. Without considering the equations describing these flows, let us note that the very important factor determining the efficiency of ion capture by an aerosol particle is the integral surface of the particle

$$S_a = 4\pi \int_0^\infty \frac{dN}{dr} r^2 \, dr.$$

This surface varies from 10^{-9} cm^2/cm^3 under the background conditions in the troposphere and stratosphere up to 10^{-4} cm^2/cm^3 in dust storms and at volcanic eruptions. The coefficients of ion capture by aerosol particles β were estimated by Brikar[15] for aerosol particles having the size of 10^{-7}–10^{-5} cm. For $a = 2\cdot 10^{-7}$ cm, the dependence of β_a on a is practically linear $\beta_a = c\,\beta_0\,a$. Here β_0 is about $0.6\cdot 10^{-6}$ $\text{cm}^{-3}\,\text{s}^{-1}$ for $a = 2\cdot 10^{-7}$ cm. The dependence of the coefficient of ion capture on the size of oppositely charged particles is very strong. The ratio of β of a charged particle to β_0 of a non-charged one varies from 1 for $a = 2\cdot 10^{-5}$ cm to 20 for $a = 0.6\cdot 10^{-6}$ cm. The use of these calculations for the actual atmospheric conditions is quite difficult because of a wide variety of atmospheric conditions, as well as polydispersity and complexity of aerosol microstructure. The ion lifetime varies from 50 to 500 s in the troposphere up to the altitude of 10 km and increases significantly at higher altitudes because of the decreasing concentrations of ions and aerosol particles. The lifetimes τ_r without aerosols and τ_a calculated by Arnold[18] for model values of the ion and aerosol concentrations are shown in Fig. 3.

The curve τ_{1a} corresponds to the background aerosol model, and τ_{2a} is for the model with a meteorite flow; curves *1*, *2*, and *3* correspond to different degrees of pollution of the troposphere.

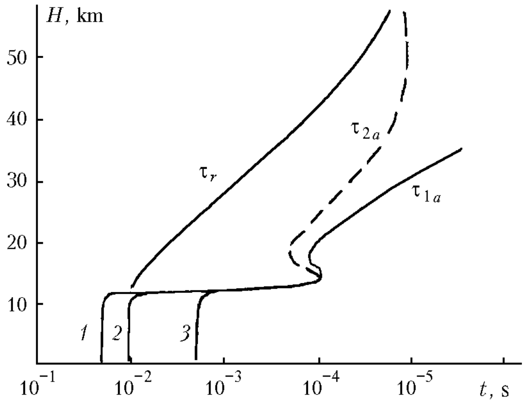

Fig. 3. Lifetimes τ_i of light ions under different external conditions as calculated in Ref. 18.

4. Structural characteristics of atmospheric aerosols

The vertical profiles of the number density and disperse composition of atmospheric aerosols were measured with balloon-borne photoelectric counters, impactors, and counters of condensation nuclei,[19–21] as well as with airborne rocket impactors.[22,23] Measurements in high latitudes are few. The largest set of the data on the vertical profile of the number density for particles of the size $a > 0.15$ μm was obtained by Rosen.[19] The disperse composition of particles was studied by Ivlev with co-workers[20,23] by the method of electron-microscope analysis of impactor samples. Figure 4 shows the experimental data on the disperse composition of aerosol particles averaged over 1980–1988. The data on the relative size distribution $\mathrm{d}N/\mathrm{d}a$ and volume distribution $\mathrm{d}V/\mathrm{d}a = 4/3\pi a^3 \mathrm{d}N/\mathrm{d}a$ at some altitudes are presented as well.

It should be noted that the function $\mathrm{d}V/\mathrm{d}a$ clearly illustrates the processes of formation and evolution of disperse structures. The function is constant for stationary transfer of aerosol from the fine state to coarser one. As larger particles are exhausted due to fast sink at insufficient inflow of fine particles or if an intense source of particles appears and the process is not still steady, the function decreases toward coarser particles. At weak sink of coarse particles as compared to inflow, the function increases with the size of particles. Hence, each maximum corresponds to the aerosol mode of a certain origin. With time, each mode shifts toward larger size and diffuses due to coagulation interaction with other modes.

The multimodal character of the distribution is well pronounced in Fig. 4*b*: the first mode with a maximum in the range from $1\cdot 10^{-2}$ to $7\cdot 10^{-2}$ μm, the second mode with a maximum in the range from $2\cdot 10^{-1}$ to $4\cdot 10^{-1}$ μm, and the third mode with a maximum in the range from 0.5 to 1 μm. Particles with the size $d < 5\cdot 10^{-3}$ μm were not analyzed because of unreliability of the data (uncertainty in the sedimentation coefficient, coagulation of particles during sampling and staying on a plate).

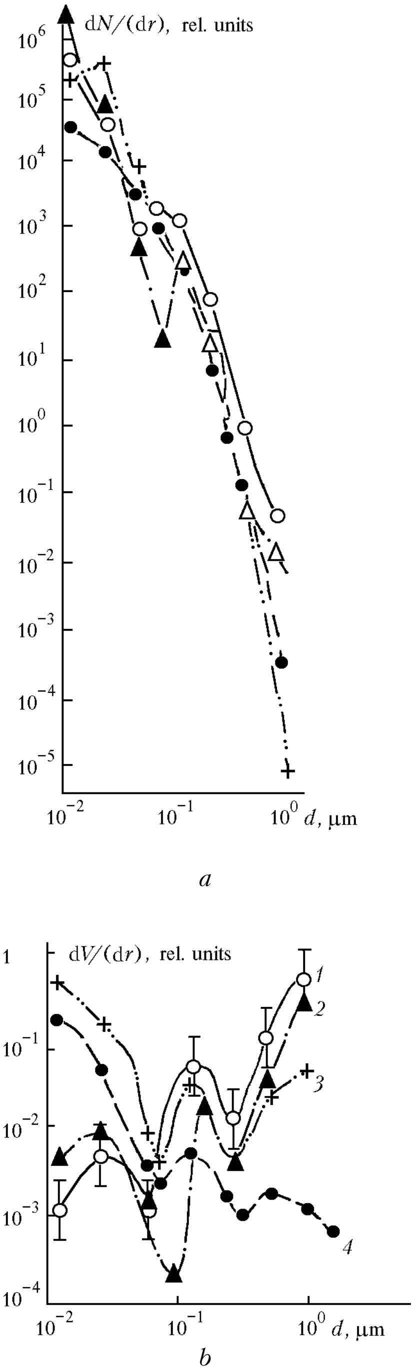

a

b

Fig. 4. Relative number $\mathrm{d}N/\mathrm{d}a$ (*a*) and volume $\mathrm{d}V/\mathrm{d}r = 4/3\pi d^3 \mathrm{d}N/\mathrm{d}a$ (*b*) aerosol particle size distributions averaged over 1982–1988 at different altitudes $h \approx 8$ (*1*), 16.5 (*2*), 25 (*3*), and 30 km (*4*).

The model vertical aerosol structure constructed based on the data of balloon-borne photoelectric counters and counters of condensation nuclei for background and post-volcanic conditions in the altitude range from 8 to 30 km is shown in Fig. 5.

It should be noted that the number density of coarse aerosol particles is noticeably increased at all altitudes and the number density of Aitken nuclei is somewhat decreased for the post-volcanic conditions roughly six months after an eruption, similar to the El Chichon eruption of 1982. Probably, Aitken nuclei are washed-out by the products of volcanic eruption due to coagulation and formed from gaseous products of volcanic eruption at high altitudes ($H > 22$ km).

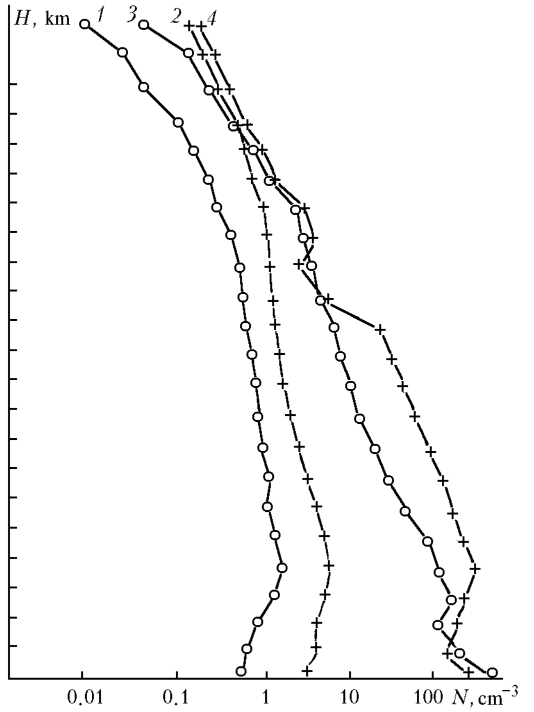

Fig. 5. Model vertical profiles of the total aerosol number density N_a (*2, 4*) and the number density N of aerosol particles with $r > 0.15$ μm (*1, 3*) for the background and post-volcanic atmosphere.

The spatial structure of aerosol in the actual atmosphere may be quite far from that shown in Fig. 5, especially, in the cases of intense emissions of dust matter (volcanoes, meteorites, explosions, etc.). Sporadic aerosol and cloud layers are formed at different altitudes when temperature isotherms and inversions preventing vertical exchange of air masses arise in the atmosphere, as well as at advective motion of air masses.

5. Thermodynamic characteristics of the atmosphere

It is obvious from the above-said that the temperature and temperature stratification of the atmosphere, as well as humidity fields and wind characteristics are the most important factors determining formation of aerosol-cloud systems as a result of phase transitions of water and other easily condensing gases, coagulation processes, and accumulation of a disperse substance as mass exchange processes in the vertical direction weaken.

The mean model temperature in the altitude range from 11 to 25 km is approximately 217 K, and it increases with the rate $\gamma = \mathrm{d}T/\mathrm{d}H = 6–7$ deg/km as the height decreases from 11 to 8 km. As the height increases $H > 25$ km, the temperature increases with the rate $\gamma = 2.5–3$ deg/km. The experimental data on the vertical profiles of relative humidity indicate that the atmosphere is dry at $H > 8$ km ($f < 20\%$). However, in some cases the humidity as well as the content of vapors of other gases, in particular, vapors easily condensing in some layers of the atmosphere, increases sharply[24] (Fig. 6).

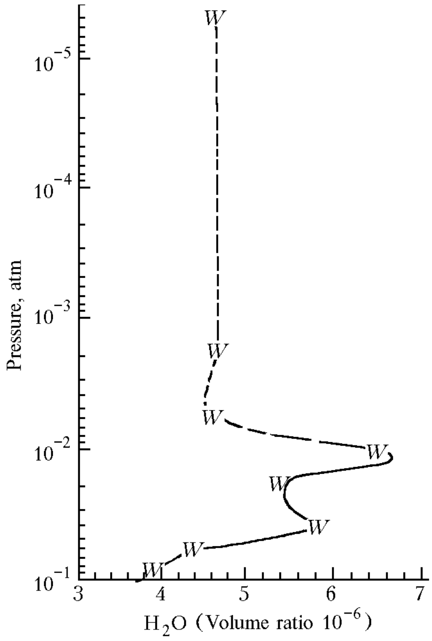

Fig. 6. Vertical profile of the volume ratio of a mixture and water vapor *W*.

The conditions for appearance of condensation or sublimation processes can be estimated based on the values of moist-adiabatic γ_{ma} (when an air element carries off the condensed moisture with its heat reserve) and pseudo-adiabatic γ_{pa} (when the whole condensate falls out of the air element under consideration) temperature lapse rates.[25]

If the temperature lapse rate in the atmosphere is higher than the moist-adiabatic one, the ascending flow leads to phase transitions of water.

The values of the pseudo-adiabatic lapse rate are given in Table 2 as functions of temperature T and pressure p (altitude H). This rate differs insignificantly from the moist-adiabatic one: $\Delta\gamma \sim 0.1$ deg/km.

Table 2. Temperature lapse rate γ_{pa}, in K/km, according to Mazin

p, hPa	T,°C								
	40	30	20	10	0	−10	−20	−30	−40
	Condensation								
1000	2.80	3.40	4.22	5.26	6.46	7.62	8.54	9.13	9.39
800	2.61	3.14	3.86	4.83	6.02	7.62	8.29	8.99	9.31
600	2.40	2.84	3.46	4.31	5.44	6.74	7.92	8.78	9.18
400	2.19	2.52	2.99	3.67	4.65	5.94	7.29	8.38	8.93
200	1.96	2.17	2.45	2.86	3.52	4.57	5.97	7.41	8.26
	Sublimation								
800	–	–	–	–	6.02	7.26	8.20	8.99	9.71
400	–	–	–	–	4.65	5.94	7.29	8.38	8.03

At the temperature lapse rate γ less than γ_{pa}, atmospheric mixing processes, including phase transitions of water, become difficult, but the conditions for accumulation of the aerosol matter and formation of aerosol-cloud layers occur. The highest temperature lapse rates are observed under the tropopause (at the altitudes from 8 to 12 km, especially in summer). The wind velocity in mid latitudes increases with height up to the tropopause due to the temperature contrasts. In the middle troposphere, narrow zones are formed, in which the west (in the Northern Hemisphere) wind achieves several hundreds kilometers per hour. These directed motion is called jet stream. It is distorted by wave processes, thus leading to formation of large-scale vortices centered in the altitude range from 8 to 12 km.

References

1. K.Ya. Kondrat'iev and G.A. Nikol'skii, in: *Solar–Terrestrial Relations, Weather, and Climate* (Mir, Moscow, 1982), pp. 354–360.
2. V.K. Roldugin and E.V. Vashenyuk, Geomagn. Aeron. **34**, No. 12, 155–157 (1994).
3. S.V. Veretenenko and M.I. Pudovkin, Geomagn. Aeron. **36**, No. 1, 153–156 (1996).
4. M.I. Pudovkin and O.M. Raspopov, Geomagn. Aeron. **32**, No. 5, 1–10 (1992).
5. M.I. Pudovkin and A.L. Morozova (Dement'eva), Geomagn. Aeron. **37**, No. 3, 84–89 (1997).
6. L.S. Ivlev, *Chemical Composition and Structure of Atmospheric Aerosols* (Leningrad State University Publishing House, Leningrad, 1982), 366 pp.
7. A.I. Rusanov, F.M. Kuni, N.I. Kochurova, and V.L. Kuz'min, in: *Problems of Thermodynamics of Heterogeneous Systems and Theory of Surface Phenomena* (Leningrad State University Publishing House, Leningrad, 1979), pp. 204–214.
8. A.I. Rusanov, Dokl. Akad. Nauk SSSR **238**, No. 4, 831–834 (1978).
9. L.S. Ivlev, in: *Physics and Chemistry of Atmospheric Aerosols*, Issue 20 (1997), pp. 54–80.
10. N.A. Fuchs, *The Mechanics of Aerosols* (Pergamon, New York, 1964), 408 pp.
11. S. Twomey, *Atmospheric Aerosols* (Elsevier, New York, 1977), 417 pp.
12. R. Jaenicke, in: *Numerical Data and Functional Relationships in Science and Technology*, *Geophysics and Space Research*, Vol. 4, *Meteorology*, Landolt-Bornstein, New. Ser. (Springer Verlag, New York, 1988), pp. 391–457.
13. V.V. Klingo, Trudy Gl. Geofiz. Obs., Issue 536, 19–24 (1991).
14. V.V. Klingo. Trudy Gl. Geofiz. Obs., Issue 536, 25–33 (1991).
15. J. Bricard and J. Pradel, in: *Aerosols Handbook* (1966) pp. 87–109.
16. S.A. Pulinets, V.V. Khegai, K.A. Boyarchuk, and A.M. Lomonosov, Usp. Fiz. Nauk **168**, No. 5, 582–589 (1998).
17. V.V. Smirnov, *Ionization in the Troposphere* (Gidrometeoizdat, St. Petersburg, 1992).
18. Arnold, Pontificae Academial Scientarum Scripta Varia **56**, 103–133 (1984).
19. J.M. Rosen, D.J. Hofmann, and J. Laby, J. Atmos. Sci. **32**, 1457–1462 (1975).
20. L.S. Ivlev, in: *Parameterization of Some Kinds of Unpremeditated and Directed Effect on the Atmosphere* (Leningrad, 1984), pp. 74–89.
21. R.P. Turko, R.C. Whitten, and O.B. Toon, Rev. of Geoph. Space Phys. **20**, No. 2, 233–279 (1982).
22. S.C. Mossop, Geochim. Cosmochim. Acta **29**, 201–207 (1965).
23. L.S. Ivlev, V.M. Zhukov, V.I. Kudryashov, and S.N. Pogorskii, Izv. Akad. Nauk SSSR **25**, No. 33, 293–301 (1989).
24. E. Nipple et al., Geophys. Res. Lett. **7**, No. 7, 489–492 (1980).
25. I.P. Mazin and A.K. Khrgian, eds., *Clouds and Cloudy Atmosphere.* Handbook (Gidrometeoizdat, Leningrad, 1989), 648 pp.